Towards Automating Diabetic Foot Monitoring

João S. Sequeira[1][0000−0002−6706−5365] and Gonçalo M. Neves[1][0000−0003−1961−0282]

Institute for Systems and Robotics/Instituto Superior Técnico, Lisbon, Portugal
joao.silva.sequeira@tecnico.ulisboa.pt
https://sites.google.com/view/joao-silva-sequeira
goncalomneves@tecnico.ulisboa.pt

Abstract. Diabetic Foot (DF) is a medical condition resulting from Diabetes, a disease with large social and economic incidence in most human societies. Monitoring the evolution of DF is essential to control the evolution of the disease, adjust therapeutics, and minimize the disturbances in the quality of life of people. The paper presents a low-cost, fully novel, system that implements standard DF medical tests, aiming at wide spreading DF testing, hence accounting for the increase in the incidence of Diabetes in general population.
DF test consists of a set of independent tests, including analysis of images of feet, sensitivity to temperature, touch and vibration, pedal pulse detection, and contact pressure of feet with the ground. The implementation of the independent devices is discussed, together with their integration in compact devices that can be used by people with minimal training and with minimal assistance from healthcare professionals.

Keywords: Diabetic Foot · Machine Learning · Deep Neural Networks · Healthcare Robotics

1 Introduction

Diabetes is a widespread disease with strong social and economic impact in most of the human societies. Monitoring its evolution is thus crucial for the definition and later adjustments of therapeutics and, most importantly, to preserve the quality of life of patients.

The novel implementation proposed in this paper relies on simple/cheap technologies, with the cost argument being a key motivation. The increase of people with Diabetes (currently 10.5% of the population has Diabetes and an estimated 11.3% will develop the condition by 2030 and 12.2% by 2045, [7], reaching 853 million to 1.31 billion by 2050, [1]) represents a relevant effort to the economies. These figures reflect a mounting burden, with the prevalence nearly doubling since 1990 [20, 8]. Monitoring and preventive assessment is thus increasingly important and automated strategies can save a significant amount of labour hence leading to economy savings.

DF testing is composed by a collection of independent tests which are applied by a healthcare technician (HT). The average time necessary for a thorough administration of the test can be in the order of 20 minutes per patient. Given the current increasing trend in the incidence of the disease, this amounts to a significant requirement of human resources. Automating the test will therefore reduce the amount of effort of healthcare professionals, which can then be used in other relevant tasks. Furthermore, it is likely to contribute to increase the DF monitoring, i.e., massifying the monitoring, by installing automated devices in social spaces such as pharmacies, nursing homes, and other healthcare spaces.

This work is part of project DFAA[1] and aims at developing completely novel automated procedures to test DF that reduce the need for constant assistance by healthcare personnel during the application of the tests. The devices were tested in colaboration with ULS-LOD[2], a partner of the DFAA project, and the entity responsible for Ethics clearances. The standard DF tests are reviewed in section 2. Preliminary results obtained with the independent devices under development are discussed. Section 3 discusses the integration of the tests in compact devices. Section 4 concludes with an assessment of the current status of the project and points to future developments.

2 Diabetic Foot Tests

Among the most serious complications are diabetic foot ulcers (DFU). Approximately 34% of people with diabetes will develop a foot ulcer during their lifetime [2]. Moreover, an estimated 80% of diabetes-related lower-leg amputations are preceded by DFUs [3, 9]. In addition, approximately 40% of patients developing a new DFU within one year of healing, with over 75% experiencing recurrence within five years [11], and the 5-year mortality rate for individuals who develop a DFU is approximately 30%, with rates exceeding 70% among those undergoing major amputations [3].

DF tests are a collection of independent tests applied to the feet of Diabetes patients to monitor the evolution of the disease and predict future events. Visual inspection of the feet assesses active ulcerations or the skin condition to predict the possibility and/or evolution of ulcerations, temperature sensitivity (not considered in this paper), touch sensitivity, vibration sensitivity, pedal pulse detection, and contact pressure of feet with the ground, form the group of tests often designated, collectively, as DF test.

Vibration and monofilament tests have been assessed in the medical literature, namely as for the frequencies used (see [13]) and foot locations where to apply them (see [24]). Similarly for the pedal pulse, which is commonly applied to assess trauma, deficit complaints (e.g., numbness, or tingling), or problems to move, and even coronary disease detection [19].

Visual inspection of the feet by healthcare professionals is prone to subjective analysis (e.g., depending on the experience of the technician performing the

[1] Diabetic Foot Automate Assessment, https://sites.google.com/view/dfaa-pex/home, an exploratory project from the Portuguese Science Foundation.

[2] Unidade Local de Saúde Loures-Odivelas, Lisbon, Portugal, a unit of the Portuguese healthcare system.

analysis). Current image analysis techniques, namely those resorting to machine learning (ML) techniques, promise to reduce this subjective component, [23].

2.1 Analysis of feet images

A visible condition of DF is the existence and severity of ulcerations of the feet. Figure 1 shows images of typical DFU. The size and color depend on the stage and severity of the ulcerations and are relevant for medical assessment. Also relevant to assess the evolution of the DF and estimate a probability/risk of evolution is the condition of the skin surrounding the ulceration.

(a) (b) (c)

Fig. 1. Sample images of typical ulcerations caused by Diabetes, Source: Kaggle dataset (public access).

Pre-conditions that can lead to the development of ulcerations include skin textures differing from the normal and situations where ulcerations have been removed, e.g., due to amputations, and the feet present mostly clean skin (see Figure 2).

(a) Medium risk (b) High risk

Fig. 2. Sample images with medium/high risk prognostic and no visible sign of ulcerations, Source: DFAA dataset (public access upon request, under CC-BY or ODC-BY licencing).

The analysis of images of feet uses two machine learning parallel pipelines (see the architecture in Figure 3). One of the pipelines aims at estimating the severity of ulcerations while the other estimates a risk of developing ulcerations given (this being a novel aspect of the project).

The training of the deep neural networks in the first pipeline used the Kaggle public dataset, for images with ulcerations. For the second pipeline training will resort to a purposefully built dataset (ongoing work), with images without ulcerations. Most datasets consist of single-view images with limited clinical diversity and lack graded risk annotations. This new, clinically validated dataset, is formed by four images of each foot.

The classification block in Figure 3, is implemented with an EfficientNetB2 net with MAP=0.8777, F1=0.9078, and AUC=0.96 (see [16]).

Risk assessment is tightly connected to explainability, i.e., information about how an ulceration is detected and what are the features that contribute the most to the result. The Grad-CAM procedure (Gradient-weighted Class Activation Mapping, [21]) has been used to interpret results of deep-learning systems by identifying the image regions that contribute the most to the final result (the sensitivity of each class to changes in the features). By overlaying the Grad-CAM heatmap on the original image, it is possible to visualize which regions the model is focusing on to make its predictions. High-intensity regions in the heat map indicate that those specific areas strongly contribute to the model's prediction.

Figure 4 shows a sample of the Kaggle dataset and the corresponding heatmap, obtained at block 20 of the EfficientNetB2. The yellow marked area (heatmap) illustrates the size of the area contributing to the ulceration, i.e., the regions in the input image that strongly influence the network's decision.

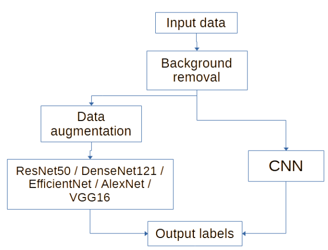

Fig. 3. Two-pipeline architecture used for image analysis

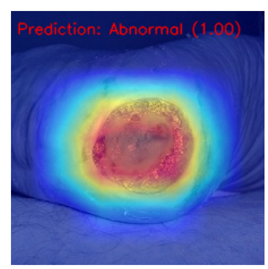

Fig. 4. Grad-CAM procedure applied to an image with an ulceration (source: DFAA project).

Examples of risk metrics can be based on (i) the area of the heatmap above a selected threshold, or (ii) the area/value of maximal gradient. The use of Grad-CAM for risk assessment has undergone a first approval screening by the MDs in project DFAA. Nevertheless, further analysis, namely on the correlation with heatmap area and MD classification, is necessary.

2.2 Touch sensitivity

The touch sensitivity is assessed by the Semmes-Weinstein 5.07 (also known as monofilament) test. The test uses a nylon filament calibrated to bend when a 10g force is applied. The healthcare technician presses the filament against specific points of the foot plantar surface (big toe and 1st, 3rd, and 5th metatarsal heads), [5], and checks if the patient is able to feel the touch as the filament bends.

The device considered in this project is shown in Figure 5. It is a rigid rod, made of plastic or wood (similar to a toothpick), connected to a micro-switch which can be connected to a computing device. The micro-switch closes when a 10g force presses the rod (an internal mechanical calibration system is used to control the closing) and a LED lights on when the calibrated force is reached. The rod can be replaced between tests to comply with hygiene recommendations. Furthermore, all the rigid components are 3D printed and hence easily replaceable.

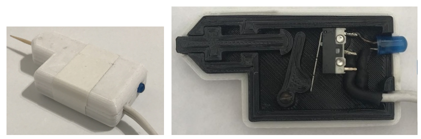

(a) External view (b) Internal view

Fig. 5. Monofilament test device. The internal view shows the lever action used to calibrate for the 10g force. An array of these devices is mounted on a linear rail allowing them to move until contact with the foot.

The test is applied for 1s at each foot location, with visual input prevented to minimize bias. The automated test application involves verifying the viability of the target areas, ensuring the skin can support the test using image processing analysis.

2.3 Vibration sensitivity

Vibration test (also called Rydel-Seiffer) is normally performed with a standard diapason (tuning fork), resonating at 128 Hz, which is set to vibrate and then a healthcare technician touches the foot of the patient and checks whether or not he/she acknowledge the vibration.

The selection of the vibration frequency to detect neuropathy depends on the region of the foot where the test is applied. For example, [10] used a 128Hz diapason on the both great toes. Similarly, [24] also use 128Hz on the first metatarsal in both feet. [12] used a 64Hz frequency and concluded that better results can be obtained by combining the vibration and the monofilament tests. Other frequencies include the ranges 4-8 Hz and 250-550 Hz, though the range 100-130 Hz is the most common one and biothesiometers/neurothesiometer devices tend to use a single frequency [13].

The current implementation (Figure 6) employs a vibration motor, commonly used in gaming interfaces, tuned to 128 Hz. It is driven by a Raspberry Pi via PWM control, allowing adjustment of the vibration frequency as needed.

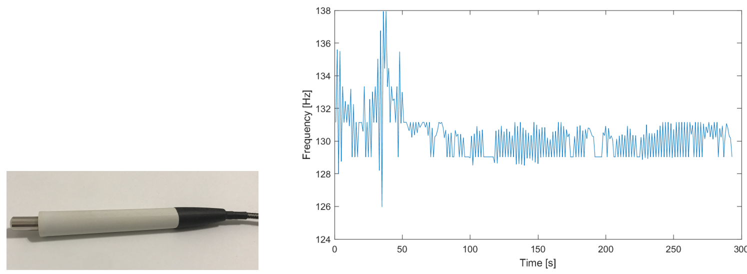

(a) (b)

Fig. 6. Device to assess vibration sensitivity (a) and sample of the signal obtained, in the range 129-130 Hz after an initial transient (b).

Similarly to the monofilament test, the vibration test must be performed with visual input prevented to minimize bias.

2.4 Pedal pulse

The measurement of pedal pulse is one of the most challenging tests to automate. Its goal is to detect blood circulation in foot arteries. Clinically, a healthcare technician locates the artery manually and, if needed, uses a Doppler ultrasound sensor [25]. Guidance documents (e.g., [14]) indicate typical probing sites: the posterior tibial and dorsalis pedis pulses. However, fine-tuning of the positioning of the sensor on the foot surface is often required, making the procedure dependent on professional expertise and difficult to automate.

Figure 7 shows two sensing devices tested to measure the pedal pulse. The Doppler ultrasound sensor (lefthand image) is commonly used in the medical area to measure blood flow. It works by detecting frequency shifts imposed by the bounding in the blood red cells [18]. The beam frequency influences the penetration and resolution of the measurement. The higher the orientation alignment between the probe and the blood flow, the higher the variation of the probe frequency. Having the ability to interpret the output (sound) of the sensor depends on listening training and personal skills [18]. An alternative principle measures the transit time of the beam that crosses the vessel (see [22]).

The infrared heart rate detector produces a signal (see Figure 8) which is a function of the pumping power/pressure of the heart, measured locally (in the pedal region). A pressure signal is proportional to the corresponding flow (as the arteries may be of small/large caliber, allowing small/large flow under the same pressure).

Using the Darcy-Weisbach equation (see [6]),

$$\Delta P = f \tfrac{L}{D} \left(\tfrac{\rho v^2}{2} \right), \qquad Q = Av \tag{1}$$

where f is a friction factor, L and D the length and internal diameter, respectively, of the pipe (artery in this case), v is the velocity of the fluid (blood), ρ

(a) Doppler ultrasound (b) Infrared heart rate detector

Fig. 7. Pedal pulse measurement devices

is the density of the fluid, g the acceleration of gravity, A is the area of a cross-section of the artery, Q the flow, and ΔP the pressure difference between two extremities of the artery[3]. It is clear that the pressure difference, ΔP is directly related to the flow, i.e., the amount of blood moving on the vessel, through its velocity.

ΔP is a spatial pressure differential, i.e., related to a spatial displacement (the endpoints of the artery), one can relate it to a time differential using the following approximation,

$$\frac{\Delta P}{L} \approx \frac{\Delta P}{v \Delta t} \approx \frac{1}{v} \frac{\mathrm{d}P}{\mathrm{d}t}$$

where a constant velocity is implicitly assumed in the artery. Replacement in (1), yields

$$\frac{1}{v} \frac{\mathrm{d}P}{\mathrm{d}t} = \frac{f}{D} \left(\frac{\rho v^2}{2} \right)$$

i.e., by computing a time derivative of the heartbeat signal one gets an estimate of the velocity of the flow. This amounts to a cheap form (no real Doppler involved) of getting information about blood flow.

Applying the aforementioned principles of mapping pressure into velocity it is possible to construct multiple variants of a Doppler sensor, i.e., by treating the pressure signal from a heartbeat sensor to sound like the signal from a real Doppler sensor. Figure 9 shows measured signals using simulated Doppler sensors based on (i) frequency shift as a function of the pedal pulse, to emulate the typical Doppler breath sound, and (ii) direct time derivative of the pedal pulse, as illustrated above.

Both variants output sound signals with similarities to the typical breath sound from medical Doppler sensors. Though for an empirical evaluation it may be important to have a sensor with expected behaviour similar to existing devices, for an automated assessment this similarity may not be relevant.

A challenge in the assessment of pedal pulses is the finding of a good location in the foot where to measure it. Multiple locations are referred to in the

[3] It is possible to argue that the Darcy-Weisbach equation is not applicable to a laminar flow. However, blood flow is likely to have regions where it is better described as a laminar flow and others as a turbulent flow, and hence we chose to keep the Darcy-Weisbach equation. Furthermore, this does not cause any inconsistency in the developed argument.

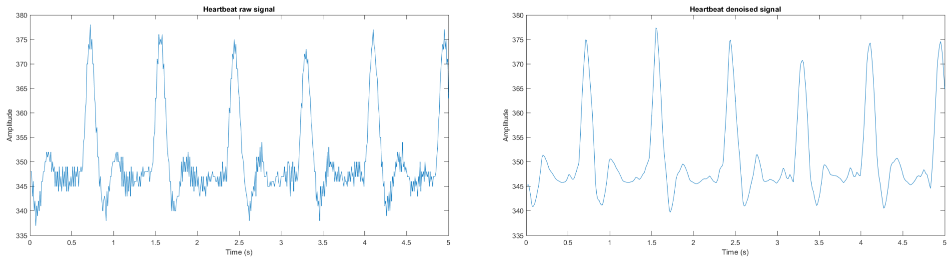

(a) Raw signal

(b) Denoised signal

Fig. 8. Heart rate signal

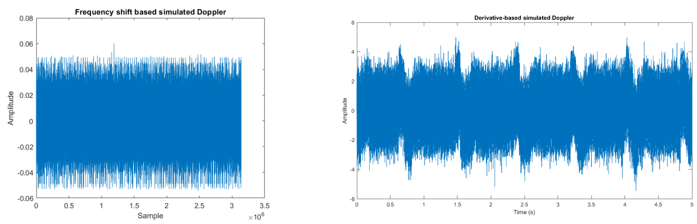

(a) Frequency shift breath emulation

(b) Pedal pulse derivative

Fig. 9. Pedal pulse measurements through simulated Doppler ultrasound techniques.

literature, e.g., dorsalis pedis pulse, measured on top of the foot and reported as difficult to obtain [15], and posterial tibial pulse, measured in the ankle bone and reported to be more reliable [4]. An automated system must select one of these options, avoiding any compromised regions of the foot, i.e., areas already ulcerated. The image analysis of Section 2.1 can be used in a first stage to discriminate among these two alternatives.

The quality of the Doppler ultrasound signal depends on the orientation of the sensor when in contact with the skin. Moreover, the use of ultrasound gel to improve the ultrasound transmission, often necessary in the DF exam, is not adequate to an automated procedure. The simulated Doppler sensors are simpler to apply, while providing information similar to the real Doppler.

2.5 Contact pressure

Figure 10 shows the device to measure the pressure of the plantar surface on the ground. The device is formed by a polycarbonate sheet where force sensitive resistors (FSR) are glued on, at relevant positions, namely following the usual medical practice (1st, 3rd, 5th metatarso, instep, big toe and heal). Measurement of the pressure through FSR has also been used in other works [17].

Although low cost FSRs are not accurate/precise load cells, the information provided is still useful for DF assessment. In this context, only a general, non-precise estimation of the plantar pressure distribution is required to identify major foot deformities or abnormal pressure patterns. Figure 10b-d shows

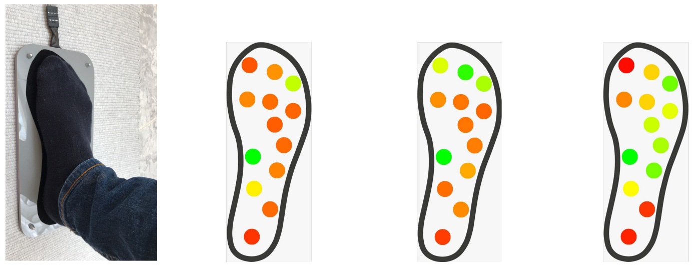

(a) Pressure plate (b) User with normal feet (c) User with big toe deformed up (d) User with big toe deformed down

Fig. 10. Measuring of the contact of the foot with the ground (device developed under DFAA project).

examples of measurements obtained in a graphic representation of the FSRs with a color scheme to show the pressure values. This test must be applied with the patient standing vertically, and it is therefore physically decoupled from the previous tests.

3 Integration

The integration of independent devices described in the previous sections is being tested following the logic presented in Figure 11, with the rigged structure for prototyping in Figure 12.

The structure contains four cameras, in fixed positions, and a 2-dof cartesian manipulator to support the vibration and monofilament devices to the foot.

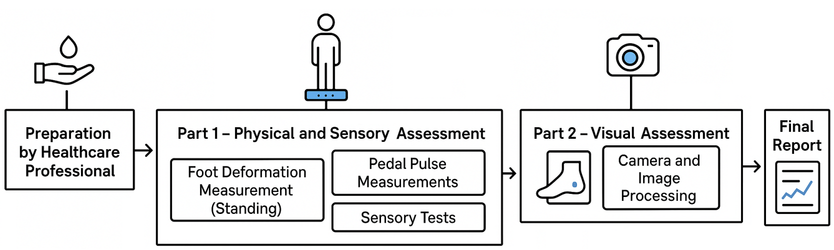

Fig. 11. Integration diagram.

Currently, the pedal pulse is applied through a passive 1D slider. The foot pressure device is kept as a separate device, since the patient should be standing, whenever possible, to ensure that the pressure applied on the device is as similar as possible to the normal pressure the foot exerts on the floor. The patient places the heel in contact with a small area, thus minimizing the uncertainty of positioning.

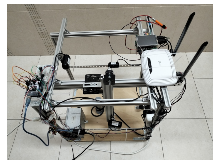

Fig. 12. Integration structure developed under the DFAA project.

4 Conclusions

The paper presented the implementations of the tests commonly used for DF assessment using low-cost technologies, aiming at expanding the application to a wider population. Massive deployment of DF tests, allowing regular, untrained, people to apply them (possibly applying the tests to themselves), is not without dangers, and hence the system proposed in this paper should run under supervision of healthcare professionals. However, the automated part of the tests will save a significant portion of the time and, in simpler cases, will be capable of the full DF assessment, producing a final report with the data collected that can be further scrutinized by healthcare professionals.

The vision for this integrated device is to combine (i) visual inspection, using a multi-camera CNN-based analysis system (the focus of this paper), (ii) foot pressure distribution, to identify abnormal load patterns, and (iii) sensory testing, to assess peripheral neuropathy.

The implementation and maintenance of the individual devices proposed in the paper is accessible to people with medium engineering skills, this also contributing to the cost effectiveness of the system, namely in what concerns maintenance. Moreover, the modular approach simplifies upgrading, e.g., as in software updates for image analysis or electronics.

This is an ongoing project. On the engineering side, future work involves completing the integration of the system and probing it under realistic conditions. On the medical side, testing each of the components and comparing them with the results obtained by certified medical devices is the main direction. Furthermore, the calibration, and reliability of all the devices will need to be thoroughly assessed in order to meet the requirements for future medical certification.

Acknowledgments. This work was supported by projects DFAA-2023.12465.PEX, from Fundação para a Ciência e Tecnologia, Portugal.

Disclosure of Interests. The authors have no competing interests to declare that are relevant to the content of this article.

References

1. International Diabetes Federation: IDF Diabetes Atlas (2025), https://www.diabetesatlas.org/, Brussels, Belgium, ISBN: 978-2-930229-96-6

2. Armstrong, D., Boulton, A., Bus, S.: Diabetic foot ulcers and their recurrence. New England Journal of Medicine **376**(24), 2367–2375 (2017). https://doi.org/10.1056/NEJMra1615439
3. Armstrong, D., Tan, T., Boulton, A., Bus, S.: Diabetic Foot Ulcers: A Review. JAMA **330**(1), 62–75 (2023). https://doi.org/10.1001/jama.2023.10578
4. Baun, J.: Practical Arterial Evaluation of the Lower Extremity. Journal of Diagnostic Medical Sonography **20**(1), 5–13 (January/February 2004). https://doi.org/10.1177/8756479303259269
5. Boulton, A., Armstrong, D., Albert, S., Frykberg, R., Hellman, R., Kirkman, M., Lavery, L., Lemaster, J., Mills, J., Mueller, M., Sheehan, P., Wukich, D.: Comprehensive Foot Examination and Risk Assessment. A report of the Task Force of the Foot Care Interest Group of the American Diabetes Association, with endorsement by the American Association of Clinical Endocrinologists. Diabetes Care **31**(8), 1679–1685 (August 2008)
6. Brown, G.: The History of the Darcy-Weisbach Equation for Pipe Flow Resistance. Environmental and Water Resources History pp. 34–43 (October 2002). https://doi.org/10.1061/40650(2003)4
7. Dysted, M., Esztergályos, B., Gautam, S., Helman, B., Pinkepank, M., Randi, A., Salim, A., Wallis, K., Jiménez, B., Ysebaert, M.: IDF Diabetes Atlas 2021. Tech. rep., International Diabetes Federation (2021), www.diabetesatlas.org
8. GBD 2021 Diabetes Collaborators: Global, regional, and national burden and trends of diabetes from 1990 to 2021, with projections to 2050 (2024). https://doi.org/10.1016/S0140-6736(23)01301-6, article id 10394
9. Hingorani, A., LaMuraglia, G., Henke, P., Meissner, H., Loretz, L., Zinszer, K., Driver, V., Frykberg, R., Carman, T., Marston, W., Mills, J.: The management of diabetic foot: A clinical practice guideline by the Society for Vascular Surgery in collaboration with the American Podiatric Medical Association and the Society for Vascular Medicine. Journal of Vascular Surgery **63**(2 Suppl), 3S–21S (2016). https://doi.org/10.1016/j.jvs.2015.10.003
10. Kästenbauer, T., Sauseng, S., Brath, H., Abrahamian, H., Irsigler, K.: The value of the Rydel-Seiffer tuning fork as a predictor of diabetic polyneuropathy compared with a neurothesiometer. Diabet Med. **21**(6), 563–567 (June 2004). https://doi.org/10.1111/j.1464-5491.2004.01205.x
11. Kitano, T., Yamada, K., Matsumoto, M., Yajima, T., Hoshina, K.: Long-term outcomes after healing of diabetic foot ulcers: a retrospective cohort study. International Journal of Lower Extremity Wounds (2025). https://doi.org/10.1177/15347346251315220
12. Lanting, S., Spink, M., Tehan, P., Vickers, S., Casey, S., Chuter, V.: Non-invasive assessment of vibration perception and protective sensation in people with diabetes mellitus: inter- and intra-rater reliability. Journal of Foot and Ankle Research **13**(3) (2020). https://doi.org/10.1186/s13047-020-0371-9
13. Lindholm, E., Löndahl, M., Fagher, K., Apelqvist, J., Dahlin, L.: Strong association between vibration perception thresholds at low frequencies (4 and 8 Hz), neuropathic symptoms and diabetic foot ulcers. PLOS ONE (February 2019). https://doi.org/10.1371/journal.pone.0212921
14. McIntosh, C.: Assessing The Vascular Status Of The Feet For Patients With Diabetes. Wound Essentials **1**, 143–147 (2006)
15. Mowlavi, A., Whiteman, J., Wilhelmi, B., Neumeister, M., McLafferty, R.: Dorsalis pedis arterial pulse: palpation using a bony landmark. Postgrad Med Journal **78**(926), 746–7 (December 2002). https://doi.org/10.1136/pmj.78.926.746

16. Neves, G., Sequeira, J.: Automatic Diabetic Foot Monitoring (2022), Preprint. Available at https://drive.google.com/file/d/1OD4eue2Oz8ZThRilPmphmVDgTrvrqJAA/view
17. Nithyaa, A., Premkumar, R., Dhivya, S., Vennila, M.: A Real Time Foot Pressure Measurement For Early Detection of Ulcer Formation In Diabetes Patients Using Labview. Procedia Engineering **64**, 1302–1309 (2013), Procs. International Conference on Design and Manufacturing IConDM 2013
18. Oglat, A., Matjafri, M., Suardi, N., Oqlat, M., Abdelrahman, M., Oqlat, A.: A Review of Medical Doppler Ultrasonography of Blood Flow in General and Especially in Common Carotid Artery. Journal of Medical Ultrasound pp. 3–13 (2018)
19. Patlola, R., Walker, C.: Pedal Pulse as an Indicator of Coronary Disease. Endovascular Today pp. 73–74 (May 2012)
20. Saeedi, P., Petersohn, I., Salpea, P., et al.: Global and regional diabetes prevalence estimates for 2019 and projections for 2030 and 2045: Results from the International Diabetes Federation Diabetes Atlas. Diabetes Research and Clinical Practice **157** (2019). https://doi.org/10.1016/j.diabres.2019.107843, article id 107843
21. Selvaraju, R., Cogswell, M., Das, A., Vedantam, R., Parikh, D., Batra, D.: Grad-CAM: Visual Explanations from Deep Networks via Gradient-based Localization (2019), arXiv:1610.02391v4 [cs.CV], this version was published also at International Journal of Computer Vision (IJCV), 2019
22. Tabrizchia, R., Pugsley, M.: Methods of blood flow measurement in the arterial circulatory system. Journal of Pharmacological and Toxicological Methods **44**, 375–384 (2000)
23. Toofanee, M., Dowlut, S., Hamroun, M., Tamine, K., Petit, V., Duong, A., Sauveron, D.: DFU-SIAM a Novel Diabetic Foot Ulcer Classification With Deep Learning. IEEE Access (September 2023). https://doi.org/10.1109/ACCESS.2023.3312531
24. Vijay, V., Snehalatha, C., Seena, R., Ramachandran, A.: The Rydel Seiffer tuning fork: an inexpensive device for screening diabetic patients with high-risk foot. Practical Diabetes Int **18**(5), 155–156 (June 2001)
25. Wang, F., Jin, P., Feng, Y., Fu, J., Wang, P., Liu, X., Zhang, Y., Ma, Y., Yang, Y., Yang, A., Feng, X.: Flexible Doppler ultrasound device forthe monitoring of blood flow velocity. Science Advances **7**(44) (October 2021). https://doi.org/10.1126/sciadv.abi9283